BUCKLING BEHAVIOR OF LONG ANISOTROPIC PLATES

SUBJECTED TO COMBINED LOADS

Michael P. Nemeth
NASA Langley Research Center
Hampton, Virginia 23681-0001

BUCKLING BEHAVIOR OF LONG ANISOTROPIC PLATES SUBJECTED TO COMBINED LOADS

Michael P. Nemeth[*]
NASA Langley Research Center
Hampton, Virginia 23681-0001

Abstract

A parametric study of the buckling behavior of infinitely long symmetrically laminated anisotropic plates subjected to combined loads is presented. The study focuses on the interaction of a stable subcritical secondary loading state of constant magnitude and a primary destabilizing load that is increased in magnitude until buckling occurs. The loads considered are uniform axial compression, pure inplane bending, transverse tension and compression, and shear. Results obtained using a special purpose nondimensional analysis that is well suited for parametric studies are presented for clamped and simply supported plates. In particular, results are presented for a $[\pm 45]_s$ graphite-epoxy laminate, and generic buckling design charts are presented for a wide range of nondimensional parameters that are applicable to a broad class of laminate constructions. These results show the effects of flexural orthotropy and flexural anisotropy on plates subjected to various combined loading conditions. An important finding of the present study is that the effect of flexural anisotropy on the buckling resistance of a plate can be increased significantly for certain types of combined loads.

Introduction

Buckling behavior of laminated plates is a topic of fundamental importance in the design of aerospace vehicle structures. Often the sizing of many subcomponents of these vehicles is determined by stability constraints in addition to strength and stiffness constraints. One subcomponent that is of practical importance in structural design is the long rectangular plate. These plates commonly appear as subcomponents of stiffened panels used for wing structures. In addition, long plates appear as subcomponents of semimonocoque shells used for fuselage and launch vehicle structures. Buckling results for infinitely long plates are important because they often provide a useful conservative estimate of the behavior of finite-length rectangular plates, and they provide information that is useful in explaining the behavior of these finite-length plates. Moreover, knowledge of the behavior of infinitely long plates can provide insight into the buckling behavior of more complex structures such as stiffened panels.

An important type of long plate that appears as a subcomponent of advanced composite structures is the symmetrically laminated plate. Symmetrically laminated plates, with plies made of the same material, remain flat during the manufacturing process and exhibit flat prebuckling deformation states. These characteristics and the amenability of these plates to structural tailoring provide symmetrically laminated plates with a significant potential for reducing structural weight of aircraft and launch vehicles. Thus, understanding the buckling behavior of symmetrically laminated plates is an important part of the search for ways to exploit plate orthotropy and anisotropy to reduce structural weight.

In many practical cases, symmetrically laminated plates exhibit specially orthotropic behavior. However, in some cases these plates exhibit anisotropy in the form of material-induced coupling between pure bending and twisting deformations. This coupling is referred to herein as flexural anisotropy and it generally yields buckling modes that are skewed in appearance, as depicted in Fig. 1. The effects of flexural orthotropy and flexural anisotropy on the buckling behavior of long rectangular plates subjected to single and combined loading conditions is becoming better understood. For example, recent in-depth parametric studies that show the effects of anisotropy on the buckling behavior of long plates subjected to compression, shear, inplane bending, and various combinations of these loads have been presented.[1,2] The results presented in these references indicate that the importance of flexural anisotropy on the buckling resistance of long plates varies with the magnitude and type of the combined loading condition. However, the extent of the influence of the combined loading condition on the importance of neglecting flexural anisotropy in a preliminary design buckling calculation is not well understood.

The objective of the present paper is to identify the effects of flexural orthotropy and, in particular, flexural anisotropy on the buckling behavior of long symmetrically laminated plates subjected combined loads. This objective is accomplished by modeling various combined loads as a primary system of destabilizing loads and a secondary system of

---

[*] Senior Research Engineer, Structural Mechanics Branch. Senior Member, AIAA.

1

subcritical loads. The primary destabilizing loads considered consist of uniform axial compression, shear, and pure inplane bending loads, and the secondary subcritical loads considered consist of transverse tension or compression and shear loads. Results are presented for plates with the two opposite long edges clamped or simply supported. A number of generic buckling curves that are applicable to a wide range of laminate constructions are also presented using the nondimensional parameters described in Refs. 1- 3.

Analysis Description

Often in preparing generic design charts for buckling of a single flat plate, a special purpose analysis is preferred over a general purpose analysis code, such as a finite element code, due to the cost and effort usually involved in generating a large number of results with a general purpose code. The results presented herein were obtained using such a special purpose analysis. The analysis details are lengthy so only a brief description of the analysis is presented herein.

Symmetrically laminated plates can have many different constructions because of the wide variety of material systems, fiber orientations, and stacking sequences that can be used to construct a laminate. A way of coping with the vast diversity of laminate constructions is to use convenient nondimensional parameters. The buckling analysis used in the proposed paper is based on the classical Rayleigh-Ritz method, and is derived explicitly in terms of the nondimensional parameters defined in Refs. 1-3. This approach was motivated by the need to conduct generic in-depth parametric studies of buckling behavior and to obtain results that indicate overall trends and the sensitivity of the results to changes in the parameters. The nondimensional parameters used in the present paper are given by

$$\alpha_{\infty} = \frac{b}{\lambda}\left(\frac{D_{11}}{D_{22}}\right)^{1/4} \qquad (1)$$

$$\beta = \frac{D_{12} + 2D_{66}}{(D_{11}\,D_{22})^{1/2}} \qquad (2)$$

$$\gamma = \frac{D_{16}}{(D_{11}^3\,D_{22})^{1/4}} \qquad (3)$$

$$\delta = \frac{D_{26}}{(D_{11}\,D_{22}^3)^{1/4}} \qquad (4)$$

where b is the plate width and λ is the half-wave length of the buckle pattern of an infinitely long plate (see Fig. 1). The subscripted D-terms are the bending

stiffnesses of classical laminated plate theory. The parameters α_{∞} and β characterize the flexural orthotropy, and the parameters γ and δ characterize the flexural anisotropy.

The loading combinations included in the analysis are uniform biaxial tension and compression, uniform shear, and eccentric inplane bending as depicted in Fig. 1. The longitudinal stress resultant N_x is partitioned in the analysis into a uniform compression part and a linearly varying part corresponding to eccentric inplane bending loads. This partitioning is given by

$$N_x = N_{xc} - N_b\left[\epsilon_0 + (\epsilon_1 - \epsilon_0)\eta\right] \qquad (5)$$

where N_{xc} denotes the intensity of the constant-valued tension or compression part of the load, and the term containing N_b defines the intensity of the eccentric inplane bending load distribution. The symbols ϵ_0 and ϵ_1 define the distribution of the inplane bending load, and the symbol η is the nondimensional coordinate given by $\eta = y/b$.

The analysis is based on a general formulation that includes combined destabilizing loads that are proportional to a positive-valued loading parameter $\bar{p}$ that is increased monotonically until buckling occurs, and independent subcritical combined loads that remain fixed at a specified load level below the point of instability. These two loading types are referred to herein as the primary (or destabilizing) and secondary (or subcritical) loading systems, respectively. In practice, the subcritical loading system is applied to a plate prior to the primary loading system with an intensity that is below the intensity that will cause the plate to buckle. Then, with the secondary loading system fixed, the primary loading system is applied by increasing the magnitude of the loading parameter until buckling occurs. This approach permits combined loading interaction to be investigated in a direct and convenient manner.

The distinction between the primary and secondary loading systems is implemented in the buckling analysis by partitioning the prebuckling stress resultants as follows

$$N_{xc} = -N_{x1}^c + N_{x2}^c \qquad (6)$$

$$N_y = -N_{y1} + N_{y2} \qquad (7)$$

$$N_{xy} = N_{xy1} + N_{xy2} \qquad (8)$$

$$N_b = N_{b1} + N_{b2} \qquad (9)$$

2

where the stress resultants with the subscript 1 constitute the primary loading system, and those with the subscript 2 constitute the subcritical loading system. The sign convention used herein for positive values of these stress resultants are shown in Fig. 1. The normal stress resultants of the primary loading system, N_{x1}^c and N_{y1} are defined to be positive-valued for compression loads. This convention results in positive eigenvalues being used to indicate instability due to compression loads.

The buckling analysis includes several nondimensional stress resultants associated with equations (6) through (9). These dimensionless stress resultants are given by

$$n_{xj}^c = \frac{N_{xj}^c\, b^2}{\pi^2 (D_{11}\, D_{22})^{1/2}} \qquad (10)$$

$$n_{yj} = \frac{N_{yj}\, b^2}{\pi^2\, D_{22}} \qquad (11)$$

$$n_{xyj} = \frac{N_{xyj}\, b^2}{\pi^2 (D_{11}\, D_{22}^3)^{1/4}} \qquad (12)$$

$$n_{bj} = \frac{N_{bj}\, b^2}{\pi^2 (D_{11}\, D_{22})^{1/2}} \qquad (13)$$

where the subscript j takes on the values of 1 and 2. In addition, the primary loading system is expressed in terms of the loading parameter $\tilde{p}$ in the analysis by

$$n_{x1}^c = L_1 \tilde{p} \qquad (14)$$

$$n_{y1} = L_2 \tilde{p} \qquad (15)$$

$$n_{xy1} = L_3 \tilde{p} \qquad (16)$$

$$n_{b1} = L_4 \tilde{p} \qquad (17)$$

where L_1 through L_4 are load factors that determine the specific form of a given primary loading system. Typically, the dominant load factor is assigned a value of 1 and all others are given as positive or negative fractions.

Nondimensional buckling coefficients used herein are given by the values of the dimensionless stress resultants of the primary loading system at the onset of buckling; i.e.,

$$K_x \equiv \left(n_{x1}^c \right)_{cr} \;\rightarrow\; K_x = \frac{\left(N_{x1}^c \right)_{cr} b^2}{\pi^2 (D_{11}\, D_{22})^{1/2}} = L_1\, \tilde{p}_{cr} \qquad (18)$$

$$K_y \equiv \left(n_{y1} \right)_{cr} \;\rightarrow\; K_y = \frac{\left(N_{y1} \right)_{cr} b^2}{\pi^2 D_{22}} = L_2\, \tilde{p}_{cr} \qquad (19)$$

$$K_s \equiv \left(n_{xy1} \right)_{cr} \;\rightarrow\; K_s = \frac{\left(N_{xy1} \right)_{cr} b^2}{\pi^2 (D_{11}\, D_{22}^3)^{1/4}} = L_3\, \tilde{p}_{cr} \qquad (20)$$

$$K_b \equiv \left(n_{b1} \right)_{cr} \;\rightarrow\; K_b = \frac{\left(N_{b1} \right)_{cr} b^2}{\pi^2 (D_{11}\, D_{22})^{1/2}} = L_4\, \tilde{p}_{cr} \qquad (21)$$

where $\tilde{p}_{cr}$ is the magnitude of the loading parameter at buckling. Positive values of the coefficients K_x and K_y correspond to uniform compression loads, and the coefficient K_s corresponds to uniform positive shear. The direction of a positive shear stress resultant acting on a plate is shown in Fig. 1. The coefficient K_b corresponds to the specific inplane bending load distribution defined by the selected values of the parameters ε_0 and ε_1.

The mathematical expression used in the variational analysis to represent the general off-centered and skewed buckle pattern is given by

$$w_N(\xi,\eta) = \sum_{m=1}^{N} \left(A_m \sin\pi\xi + B_m \cos\pi\xi \right) \Phi_m(\eta) \qquad (22)$$

where $\xi = x/\lambda$ and $\eta = y/b$ are nondimensional coordinates, w_N is the out-of-plane displacement field, and A_m and B_m are the unkown displacement amplitudes. In accordance with the Rayleigh-Ritz method, the basis functions $\Phi_m(\eta)$ are required to satisfy the kinematic boundary conditions on the plate edges at $\eta = 0$ and 1. For the simply supported plates the basis functions used in the analysis are given by

$$\Phi_m(\eta) = \sin m\pi\eta \qquad (23)$$

for values of $m = 1, 2, 3, ..., N$. Similarly, for the clamped plates, the basis functions are given by

$$\Phi_m(\eta) = \cos(m-1)\pi\eta - \cos(m+1)\pi\eta \qquad (24)$$

Algebraic equations governing the buckling behavior of infinitely long plates are obtained by substituting the series expansion for the buckling mode given by equation (22) into the second variation of the total potential energy and then computing the integrals appearing in the second variation in closed form. The resulting equations constitute a generalized eigenvalue

3

problem that depends on the aspect ratio of the buckle pattern λ/b (see Fig. 1) and the nondimensional parameters and nondimensional stress resultants defined herein. The smallest eigenvalue of the problem corresponds to buckling and is found by specifying a value of λ/b and solving the corresponding generalized eigenvalue problem for its smallest eigenvalue. This process is repeated for successive values of λ/b until the overall smallest eigenvalue is found.

Results obtained using the analysis described herein have been compared with other results for isotropic, orthotropic, and anisotropic plates obtained using other analysis methods. These comparisons are discussed in Refs. 1 and 2, and in every case the analysis described herein was found to be in good agreement with the results obtained from other analyses.

Results and Discussion

Results are presented herein for clamped and simply supported plates loaded by various combinations of axial compression, transverse tension or compression, pure inplane bending, and shear. For loading cases involving shear, a distinction is made between positive and negative shear loads whenever flexural anisotropy is present. A positive shear load corresponds to the shear loads shown in Fig. 1. No distinction between positive and negative pure inplane bending loads is necessary for flexurally anisotropic plates.

Results are presented first for $[\pm45]_s$ flexurally anisotropic plates that show how significant the interaction between the plate anisotropy and the type of combined loading can be for an actual laminate. This thin laminate is representative of spacecraft structural components and is made of a typical graphite-epoxy material with a longitudinal modulus $E_1 = 127.8$ GPa (18.5×10^6 psi), a transverse modulus $E_2 = 11.0$ GPa (1.6×10^6 psi), an inplane shear modulus $G_{12} = 5.7$ GPa (0.832×10^6 psi), a major Poisson's ratio $v_{12} = 0.35$, and a nominal ply thickness of 0.127mm (0.005 in.).

Generic results are presented next, in terms of the nondimensional parameters described herein, for a range of parameters that is applicable to a broad class of laminate constructions. The range of each nondimensional parameters used herein is given by $0.1 \leq \beta \leq 3.0$, $0 \leq \gamma \leq 0.6$, and $0 \leq \delta \leq 0.6$. A value of 0.6 for γ and δ corresponds to a highly anisotropic plate. For isotropic plates, $\beta = 1$ and $\gamma = \delta = 0$. Moreover, for plates without flexural anisotropy, $\gamma = \delta = 0$. Values of these parameters corresponding to several practical laminates are given in Refs. 1 and 2.

To simplify the presentation of the fundamental generic behavioral trends, results are presented herein for plates in which γ and δ have equal values. However, this approach is applicable to laminates such as a $[+35/-15]_s$ laminate made of the typical graphite-epoxy material described herein. For this laminate, $\beta = 1.95$, $\gamma = 0.52$, and $\delta = 0.51$. Furthermore, results showing the effects of α_∞, or equivalently $(D_{11}/D_{22})^{1/4}$, on the buckling coefficients are not presented herein since it has been shown in Refs. 1 and 2 that variations in this parameter only affect the critical value of the buckle aspect ratio λ/b and not the buckling coefficient. A value of $(D_{11}/D_{22})^{1/4} = 1$ was used in all the calculations presented herein. For clarity, the compression, shear, and inplane bending buckling coefficients, defined by Eqns. (18) (20), and (21), respectively, are expressed as $K_x\big|_{\gamma=\delta=0}$, $K_s\big|_{\gamma=\delta=0}$, and $K_b\big|_{\gamma=\delta=0}$ when describing the generic results for which flexural anisotropy is neglected in the analysis.

Results for $[\pm45]_s$ Plates

Results are presented in Fig. 2 for a clamped $[\pm45]_s$ plate subjected to a destabilizing uniform uniaxial compression load. In addition, results are presented for a combined loading condition consisting of uniform axial compression and either a uniform transverse tension or a compression subcritical load. Similar results are presented in Fig. 3 for a corresponding plate in which the destabilizing load is a uniform shear load. In these figures, the minimum value of the loading parameter found by solving the generalized eigenvalue problem for a given value of λ/b is shown for values of $0 \leq \lambda/b \leq 2$. Moreover, the magnitude of the subcritical transverse load is indicated in the figures by the value of the nondimensional stress resultant n_{y2} defined by Eqn. (11). A limiting value of the subcritical load given by $n_{y2} = -4$ corresponds to a wide column buckling mode. The dashed lines shown in the figures correspond to the actual solutions to the generalized eigenvalue problem that are obtained when flexural anisotropy is included in the analysis. In contrast, the solid lines correspond to the solutions that are obtained when flexural anisotropy is neglected in the analysis. The overall minimum value of the loading parameter for each of the curves is indicated by filled circles and these values correspond to the values of the buckling coefficients for each curve. The corresponding values of λ/b are the critical values of the buckle aspect ratio.

4

The results presented in Fig. 2 indicate that neglecting the flexural anisotropy in a buckling analysis of a pure compression-loaded plate ($n_{y2} = 0$) overestimates the buckling coefficient (minimum loading parameter) by 30% of the anisotropic buckling load, and slightly overestimates the critical value of the buckle aspect ratio λ/b. For a transverse tension subcritical load given by $n_{y2} = 3.5$ (87.5% of the magnitude for a wide column buckling mode), the results show that the effect of the flexural anisotropy becomes slightly less important; i.e., the buckling coefficient is overestimated by 22% for this case. Neglecting the anisotropy for this case also slightly overestimates the critical value of the buckle aspect ratio. However, for a subcritical transverse compression load given by $n_{y2} = -3.5$, the buckling coefficient is overestimated by 76% when the flexural anisotropy is neglected in the analysis, and the critical value of the buckle aspect ratio is slightly underestimated.

The results shown in Fig. 3 for a shear-loaded plate with a transverse tension or compression subcritical load and the results shown in Fig. 2 indicate that neglecting the flexural anisotropy in the buckling analysis is much more pronounced for the shear-loaded plate than for the corresponding compression-loaded plate. In particular, the results presented in Fig. 3 indicate that neglecting the flexural anisotropy in the buckling analysis of a pure shear-loaded plate ($n_{y2} = 0$) overestimates the buckling coefficient by 97% of the anisotropic buckling load as compared to 30% for the corresponding compression-loaded plate. For a transverse tension subcritical load given by $n_{y2} = 3.5$, the results for the shear-loaded plate predict that the buckling coefficient is overestimated by 75%. More significantly, for a transverse compression subcritical load given by $n_{y2} = -3.5$, the results predict that the shear buckling coefficient is overestimated by 209% when the flexural anisotropy is neglected in the analysis.

Results similar to the results presented in Figs. 2 and 3 are presented in Figs. 4 and 5 for a $[\pm 45]_s$ plate that is loaded by either uniform axial compression or pure inplane bending, respectively. Two groups of curves are shown in the figures that correspond to plates without a subcritical load and with either a positive or negative subcritical shear load with a magnitude equal to 75% of the corresponding shear buckling coefficient K_s (see Eqn. 20). For the cases in which the anisotropy is included in the analysis, the buckling coefficients for positive and negative shear loads are given by $K_s = 6.12$ and $K_s = -17.16$, respectively. For the cases in which the anisotropy is neglected, the buckling coefficients for positive and negative shear loads are given by $K_s =$

12.03 and $K_s = -12.03$, respectively. The results shown in Figs. 4 and 5 include the effects of neglecting the anisotropy in the calculation of the subcritical load n_{xy2} as well as the actual calculation of the buckling coefficient.

The results shown in Figs. 4 and 5 indicate that neglecting the flexural anisotropy in a buckling analysis of the plate subjected to only uniform axial compression or pure inplane bending ($n_{xy2} = 0$) overestimates the buckling coefficient by approximately 30% of the anisotropic buckling load, and the critical value of the buckle aspect ratio is slightly overestimated. For the subcritical positive shear load with $n_{xy2} = 0.75K_s$, the results predict that the buckling coefficient is overestimated by about 84% and 66% of the anisotropic buckling coefficient for the uniform axial compression and pure inplane bending loads, respectively. Moreover, for both loading conditions, the critical value of the buckle aspect ratio is also slightly overestimated when the anisotropy is neglected in the analysis. In contrast, for the subcritical negative shear load with $n_{xy2} = 0.75K_s$, the results predict that the buckling coefficient is underestimated by about 26% and 16% of the anisotropic buckling coefficient for the uniform axial compression and pure inplane bending loading conditions, respectively. In addition, the critical value of the buckle aspect ratio is slightly underestimated for the uniform axial compression load and slightly overestimated for the pure inplane bending load when the flexural anisotropy is neglected in the analysis.

Generic Effects of Flexural Orthotropy

Results are presented in Figs. 6 through 10 that show the generic effects of plate flexural orthotropy on the buckling coefficients of clamped and simply supported plates with $\gamma = \delta = 0$. The results in Figs. 6, 7, and 8 are for plates subjected to a subcritical transverse tension or compression load and a destabilizing uniform axial compression load, pure inplane bending load, and shear load, respectively. Similarly, the generic effects of flexural orthotropy on plates subjected to a subcritical shear load and a uniform axial compression load or a pure inplane bending load are shown in Figs. 9 and 10, respectively. The results in Figs. 9 and 10 are also applicable to plates loaded in negative shear since the shear buckling coefficients for identical plates loaded in positive or negative shear have the same magnitude when anisotropy is neglected in the calculations. Two sets of curves are shown in Figs. 6 through 10 for values of the orthotropic parameter $\beta = 0.5, 1, 1.5, 2, 2.5,$ and 3. The solid curves correspond to results for clamped plates and the dashed curves are for simply supported plates. These curves show the

5

buckling coefficient as a function of the nondimensional transverse load n_{y2} in Figs. 6 through 8, and as a function of the nondimensional shear load n_{xy2} in Figs. 9 and 10.

The results presented in Figs. 6 through 10 indicate that the orthotropic buckling coefficients ($\gamma = \delta = 0$) increase substantially as the orthotropic parameter β increases. Furthemore, the results in Figs. 6 through 8 indicate that as the subcritical transverse load increases through positive values (increasing tension), the buckling coefficients increase substantially. This trend is shown to be more pronounced for the shear-loaded plates than for the compression-loaded plates or the plates loaded by pure inplane bending. Moreover, the increase in buckling coefficient with increasing subcritical tension load is predicted to be slightly more pronounced for the simply supported plates than for the clamped plates. The results presented in Figs. 9 and 10 for the plates with subcritical shear loads indicate a substantial reduction in the buckling coefficient as the magnitude of the nondimensional shear load increases. In addition, the results also predict this trend to be slightly more pronounced for the simply supported plates than for the clamped plates.

Interaction of Flexural Anisotropy and Loading

Results are presented in Figs. 11 through 18 that show the generic effects of plate flexural anisotropy and combined loading condition on the buckling coefficients of clamped and simply supported plates. In particular, the results shown in Figs. 11, 12, 13, and 14 are for plates subjected to a subcritical transverse tension or compression load and uniform axial compression, pure inplane bending, and shear destabilizing loads, respectively. In addition, the results shown in Figs. 15, 16, 17, and 18 are for plates subjected to a subcritical shear load and uniform uniaxial compression and pure inplane bending, respectively. The results in Figs. 15 and 17 are for a positive subcritical shear load, and the results in Figs. 16 and 18 are for a negative subcritical shear load. In each of Figs. 11 through 18, the ratio of the anisotropic buckling coefficient to the corresponding orthotropic buckling coefficient computed with $\gamma = \delta = 0$ (see Figs. 6 through 10) is given as a function of the orthotropic parameter β for discrete equal values of the anisotropic parameters ($\gamma = \delta$) ranging from 0.1 to 0.6. For each value of $\gamma = \delta$ given in Figs. 11 through 14, three curves are presented. The solid lines correspond to a value of the nondimensional transverse load $n_{y2} = 0$ used in the calculations (no subcritical load). Similarly, the finely dashed and coursely dashed lines correspond to values of $n_{y2} = -0.5$ (compression) and 0.5 (tension), respectively, for the simply supported plates and to values of $n_{y2} = -2$ (compression) and 2

(tension), respectively, for the clamped plates. The magnitudes of these values correspond to 50% of K_y, the buckling coefficient corresponding wide-column collapse ($K_y = 1$ and 4 for simply supported and clamped plates, respectively). For each value of $\gamma = \delta$ given in Figs. 15 through 18, four curves are presented. The solid lines correspond to the value of the nondimensional shear load $n_{xy2} = 0$ (no subcritical load). Similarly, the finely dashed, moderately dashed, and coursely dashed lines correspond to values of $n_{xy2} = 0.25K_s$, $0.5K_s$, and $0.8K_s$, respectively, where K_s is the shear buckling coefficient. More specifically, K_s is the positive shear buckling coefficient in Figs. 15 and 17, and the negative shear buckling coefficient in Figs. 16 and 18. For each case, the shear buckling coefficient is a function of β, γ, and δ.

The results for plates subjected to a subcritical transverse tension or compression load and uniform uniaxial compression presented in Figs. 11 and 12 show that the anisotopic buckling coefficient is always less than the corresponding orthotropic buckling coefficient for the full range of parameters considered. In addition, these results predict that the effects of neglecting anisotropy are more pronounced for the plates with the transverse compression loads than for the plates with no subcritical load ($n_{y2} = 0$) or a transverse tension load. Moreover, these results predict that this trend is slightly more pronounced for the clamped plates than for the simply supported plates. The results also predict that the reduction in buckling coefficient due to anisotropy is generally larger for the clamped plates with $n_{y2} = -2$ (transverse compression at a magnitude of 50% of the wide column buckling coefficient) than for the corresponding simply supported plates. However, the results also predict that the reduction in buckling coefficient due to anisotropy is generally smaller for the clamped plates with $n_{y2} = 0$ or 2 (transverse tension at a magnitude of 50% of the wide column buckling coefficient) than for the corresponding simply supported plates.

The results for simply supported plates subjected to a subcritical transverse tension or compression load and pure inplane bending presented in Fig. 13, and corresponding results for clamped plates not presented herein, also show that the anisotopic buckling coefficient is always less than the corresponding orthotropic buckling coefficient for the full range of parameters considered. These results also predict that the effects of neglecting anisotropy are more pronounced for plates with a transverse compression load than for plates with $n_{y2} = 0$ or the transverse tension load, but not to the extent that is exhibited by the corresponding plates with the uniaxial compression

6

load. Moreover, these results predict that this trend is slightly more pronounced for clamped plates than for simply supported plates, but not to the extent that is predicted for the corresponding plates with a uniaxial compression load. Furthermore, like the plates with a uniaxial compression load, the results also predict that the reduction in buckling coefficient due to anisotropy is generally larger for clamped plates with $n_{y2} = -2$ (transverse compression) than for the corresponding simply supported plates. Similarly, the results also predict that the reduction in buckling coefficient due to anisotropy is generally smaller for clamped plates with $n_{y2} = 0$ or 2 (transverse tension) than for the corresponding simply supported plates.

The results for simply supported plates subjected to a subcritical transverse tension or compression load and a positive shear load presented in Fig. 14 and corresponding results for clamped plates not presented herein also show that the anisotropic buckling coefficient is always less than the corresponding orthotropic buckling coefficient. However, these results also show that this trend is reversed for negative shear loads. These results also predict that the effects of neglecting anisotropy are generally more pronounced for plates with transverse compression loads than for plates with $n_{y2} = 0$ or with transverse tension loads, but not to the extent that is exhibited by the corresponding plates with uniaxial compression loads and slightly more than the corresponding plates loaded by pure inplane bending. Moreover, these results predict that this trend is also slightly more pronounced for clamped plates than for simply supported plates. Furthermore, like the plates with the uniaxial compression loads, the results predict that the reduction in buckling coefficient due to anisotropy is generally larger for clamped plates loaded in positive shear and with $n_{y2} = -2$ (transverse compression) than for the corresponding simply supported plates. Similarly, the results also predict that the reduction in buckling coefficient due to anisotropy is generally smaller for the clamped plates loaded in positive shear and with $n_{y2} = 0$ or 2 (transverse tension) than for the corresponding simply supported plates. For the plates loaded by negative shear, these trends are reversed. Overall, the results presented in Figs. 11 through 14 indicate that plates loaded by positive shear typically exhibit substantially larger reductions in the buckling coefficient when flexural anisotropy is neglected in the analysis than the corresponding plates loaded by uniform axial compression or pure inplane bending. In contrast, the results for plates loaded by negative shear predict sizeable increases in the buckling coefficients when the flexural anisotropy is included in the calculations.

The results presented in Fig. 15 for simply supported plates loaded by uniform axial compression and a positive subcritical shear load, and the results obtained for the corresponding clamped plates, predict monotonic reductions in buckling coefficient with increasing values of the anisotropic parameters. This same trend is also predicted for increasing magnitudes of the positive shear load as indicated by the four different line types shown in Fig. 15. Moreover, these results show that the reductions in buckling coefficients are slightly more pronounced for the simply supported plates than for the clamped plates. More importantly, these results indicate that the reduction in buckling coefficient associated with neglecting anisotropy in the calculations is substantially larger when the positive shear load is larger than approximately 50% of the corresponding shear buckling load.

The results shown in Fig. 16 for simply supported plates loaded by uniform axial compression and a negative subcritical shear load, and results obtained for corresponding clamped plates, predict monotonic reductions in buckling coefficient with increasing values of the anisotropic parameters for the values of $n_{xy2} = 0$ and $0.25K_s$. However, for the larger values of n_{xy2}, the results predict increases in buckling coefficient with increasing values of the anisotropic parameters as anticipated from the previous results presented herein. This seemingly unusual trend for the negative shear load is a manifestation of the phase shift in the compression-shear buckling interaction curves caused by flexural anisotropy that has been reported in Ref. 1. In addition, these results show this trend to be slightly more pronounced for clamped plates than for simply supported plates. Furthermore, these results indicate that the importance of anisotropy on the buckling resistance changes dramatically with the magnitude of a negative subcritical shear load.

Results similar to those presented in Fig. 15 are presented in Fig. 17 for simply supported plates loaded by pure inplane bending and a positive subcritical shear load. These results, and results obtained for corresponding clamped plates, also predict monotonic reductions in buckling coefficient with increasing values of the anisotropic parameters and increasing magnitudes of a positive shear load. However, these results show that the reductions in buckling coefficient are practically the same for the simply supported and clamped plates. The results also indicate that the reduction in buckling coefficient associated with neglecting anisotropy in the calculations is substantially larger when a positive shear load is larger than approximately 50% of the corresponding shear buckling load. Comparing the results in Figs. 15 and 17 suggests that the reductions in buckling coefficient due to neglecting flexural anisotropy is slightly more pronounced for plates loaded by uniform axial compression than for those loaded by pure inplane bending, particularly for the larger magnitudes of a subcritical shear load.

7

Results similar to those presented in Fig. 16 are presented in Fig. 18 for simply supported plates loaded by pure inplane bending and a negative subcritical shear load. These results, and results obtained for corresponding clamped plates, also predict monotonic reductions in buckling coefficient with increasing values of the anisotropic parameters for the values of $n_{xy2} = 0$ and $0.25K_s$. Unlike the results for compression loaded plates, the results in Fig. 18 also predict monotonic reductions in buckling coefficient with increasing values of the anisotropic parameters for $n_{xy2} = 0.5K_s$. For $n_{xy2} = 0.8K_s$, the results predict increases in buckling coefficient with increasing values of the anisotropic parameters. This unusual trend for a negative shear load is also a manifestation of the phase shift in the pure inplane bending-shear buckling interaction curves caused by flexural anisotropy that has been reported in Ref. 2. Moreover, the difference between the trends for plates loaded by negative shear and pure inplane bending or uniform axial compression is manifested by the pronounced difference in shape of the corresponding buckling interaction curves presented in Refs. 1 and 2. The results for the plates loaded by pure inplane bending also show the trends described above to be slightly more pronounced for the clamped plates than for the simply supported plates. Comparing the results in Figs. 16 and 18 also suggests that the change in buckling coefficient due to the interaction between flexural anisotropy and the magnitude of negative shear is substantially more pronounced for plates loaded by uniform axial compression than for those loaded by pure inplane bending.

Concluding Remarks

A parametric study of the buckling behavior of infinitely long symmetrically laminated anisotropic plates subjected to combined loads has been presented. A special purpose nondimensional analysis that is well suited for parametric studies of clamped and simply supported plates has been described and its key features have been discussed. The results presented herein have focused on the interaction of a stable subcritical secondary loading state and a primary destabilizing loading state. The interaction of uniform axial compression, pure inplane bending, transverse tension and compression, and shear loads with plate flexural anisotropy and orthotropy have been examined. In particular, results have been presented for $[\pm 45]_s$ thin graphite-epoxy laminates that are representative of spacecraft structural components. In addition, a number of generic buckling results have been presented that are applicable to a broad class of laminate constructions, and that show explicitly the effects of flexural orthotropy and flexural anisotropy on plate buckling behavior under combined loads.

The most important finding of the present study is that the importance of flexural anisotropy on the buckling behavior of a long plate is strongly dependent on the type of combined load applied and its magnitude. Specifically, the results presented herein show that significant errors (on the order of 100%) can be made calculating buckling coefficients of plates subjected to combined loads when flexural anisotropy is neglected. Overall, the results presented herein show that the buckling coefficients increase significantly as the orthotropic parameter β increases, and decrease significantly as the anisotropic parameters $(\gamma = \delta)$ increase for all load combinations considered except those involving negative shear loads. For this loading case, the trend is generally reversed. The results presented herein also generally show that the effects of plate anisotropy are more pronounced for clamped plates than for simply supported plates subjected to combined loads.

References

1. Nemeth, M. P., "Buckling Behavior of Long Symmetrically Laminated Plates Subjected to Combined Loads," NASA TP 3195, May 1992.

2. Nemeth, M. P., "Buckling Behavior of Long Symmetrically Laminated Plates Subjected to Compression, Shear, and Inplane Bending Loads," AIAA Journal, Vol. 30, No. 12, December 1992, pp. 2959-2965.

3. Nemeth, M. P., "Importance of Anisotropy on Buckling of Compression-Loaded Symmetric Composite Plates," AIAA Journal, Vol. 24, No. 11, November 1986, pp. 1831-1835.

a) Primary loading system

b) Secondary loading system
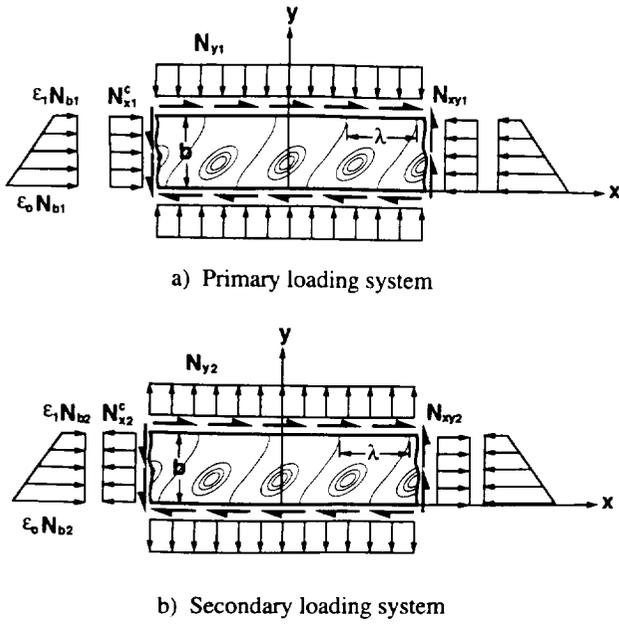
Fig. 1 Sign convention for positive-valued stress resultants $(\varepsilon_0 > \varepsilon_1 > 0)$.
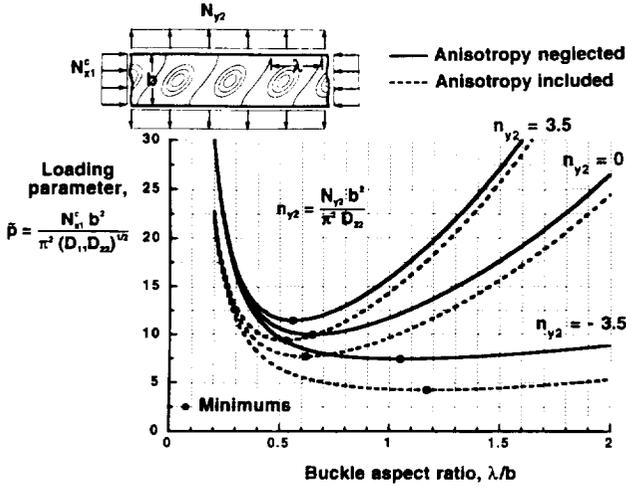

Fig. 2 Buckling results for clamped $[\pm 45]_s$ plates subjected to axial compression and subcritical transverse tension or compression loads.
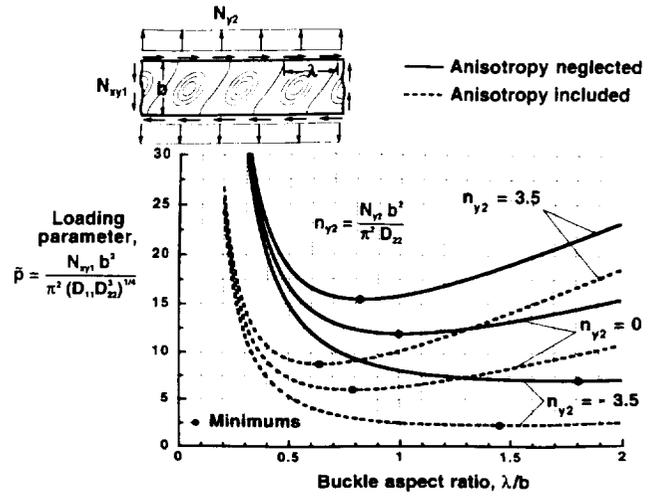

Fig. 3 Buckling results for clamped $[\pm 45]_s$ plates subjected to shear and subcritical transverse tension or compression loads.
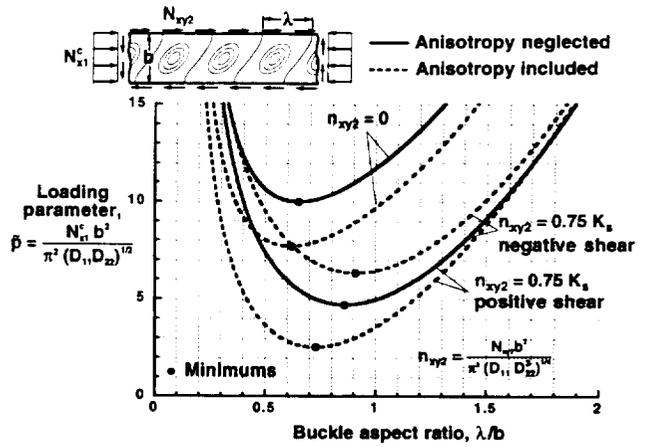

Fig. 4 Buckling results for clamped $[\pm 45]_s$ plates subjected to axial compression and subcritical shear loads.
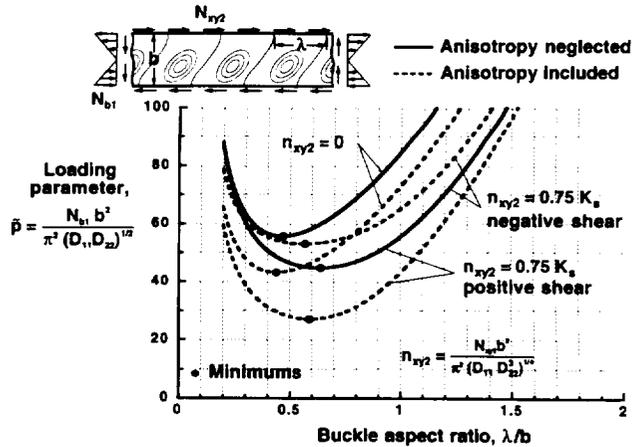
Fig. 5 Buckling results for clamped $[\pm 45]_s$ plates subjected to pure inplane bending and subcritical shear loads.

9
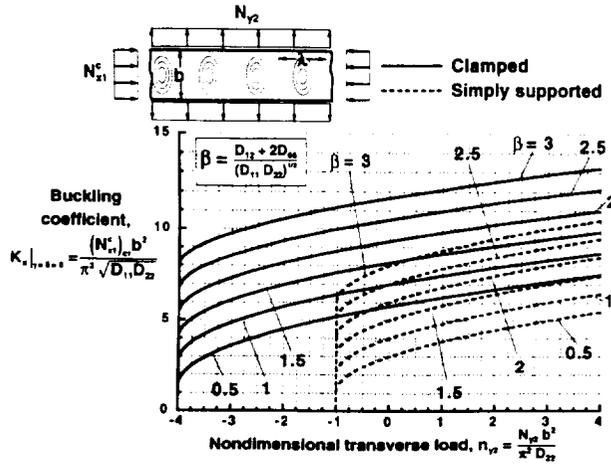
Fig. 6 Effects of orthotropic parameter β on buckling interaction curves for specially orthotropic plates (γ = δ = 0) subjected to axial compression and subcritical transverse tension or compression loads.
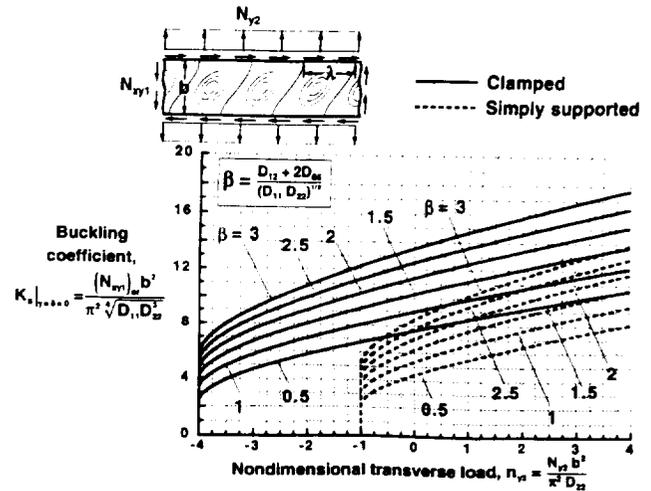
Fig. 7 Effects of orthotropic parameter β on buckling interaction curves for specially orthotropic plates (γ = δ = 0) subjected to pure inplane bending and subcritical transverse tension or compression loads.


Fig. 8 Effects of orthotropic parameter β on buckling interaction curves for specially orthotropic plates (γ = δ = 0) subjected to shear and subcritical transverse tension or compression loads.
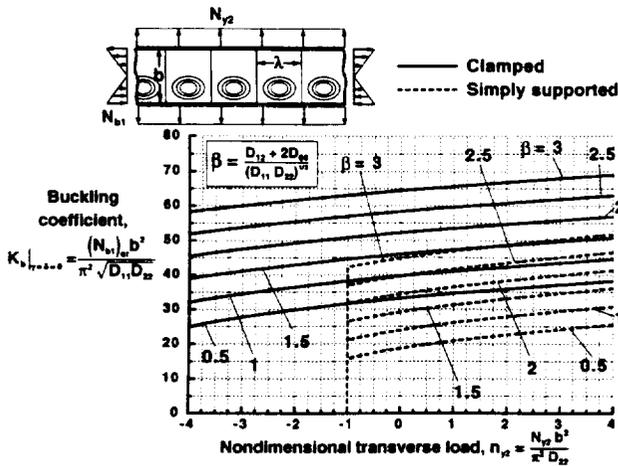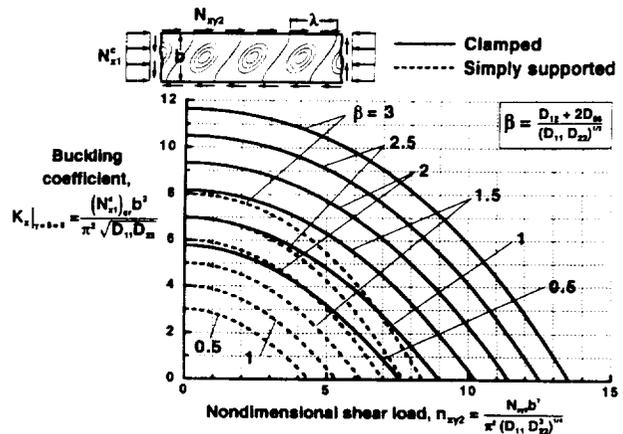
Fig. 9 Effects of orthotropic parameter β on buckling interaction curves for specially orthotropic plates (γ = δ = 0) subjected to axial compression and subcritical shear loads.
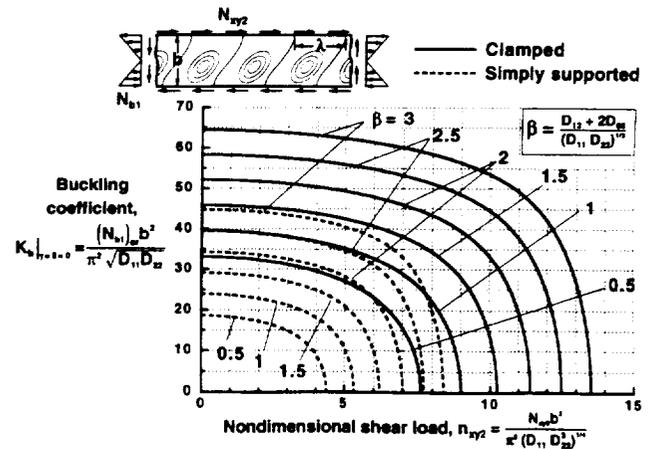
Fig. 10 Effects of orthotropic parameter β on buckling interaction curves for specially orthotropic plates (γ = δ = 0) subjected to pure inplane bending and subcritical shear loads.

10
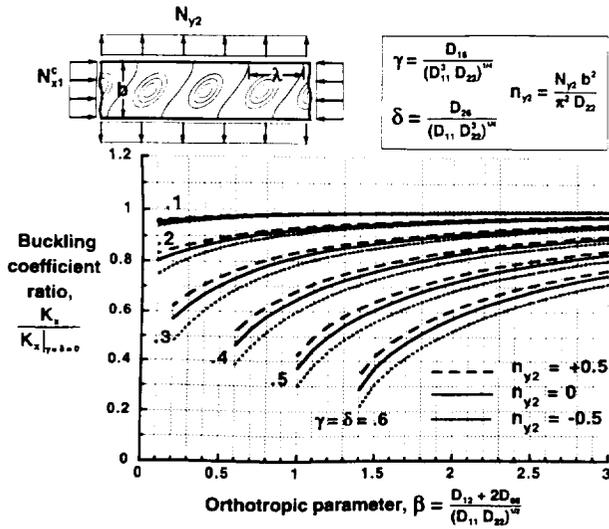
Fig. 11 Effects of orthotropic parameter β and anisotropic parameters γ and δ on buckling coefficients for simply supported plates subjected to axial compression and subcritical transverse tension or compression (n_{y2}) loads.
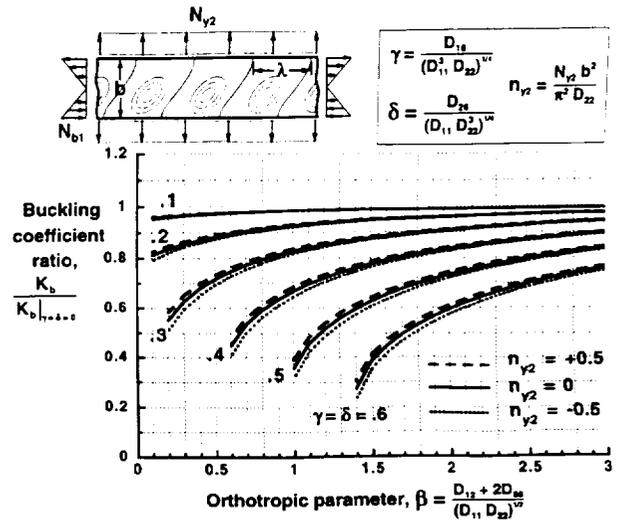

Fig. 13 Effects of orthotropic parameter β and anisotropic parameters γ and δ on buckling coefficients for simply supported plates subjected to pure inplane bending and subcritical transverse tension or compression (n_{y2}) loads.
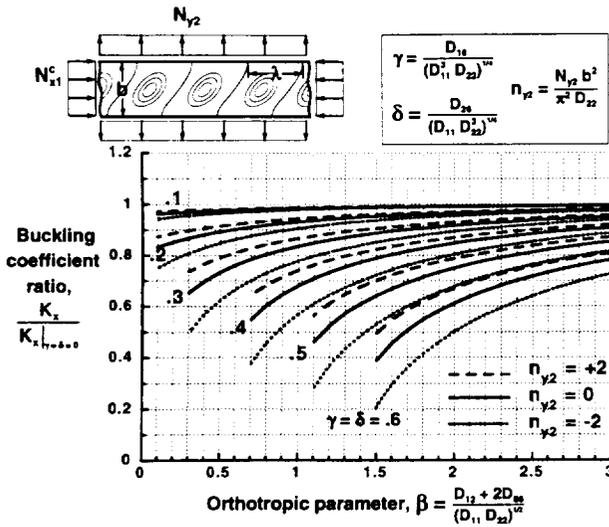
Fig. 12 Effects of orthotropic parameter β and anisotropic parameters γ and δ on buckling coefficients for clamped plates subjected to axial compression and subcritical transverse tension or compression (n_{y2}) loads.
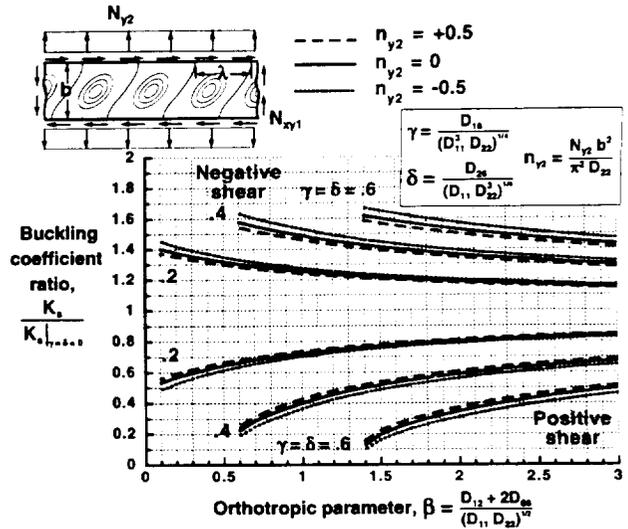
Fig. 14 Effects of orthotropic parameter β and anisotropic parameters γ and δ on buckling coefficients for simply supported plates subjected to shear and subcritical transverse tension or compression (n_{y2}) loads.

11
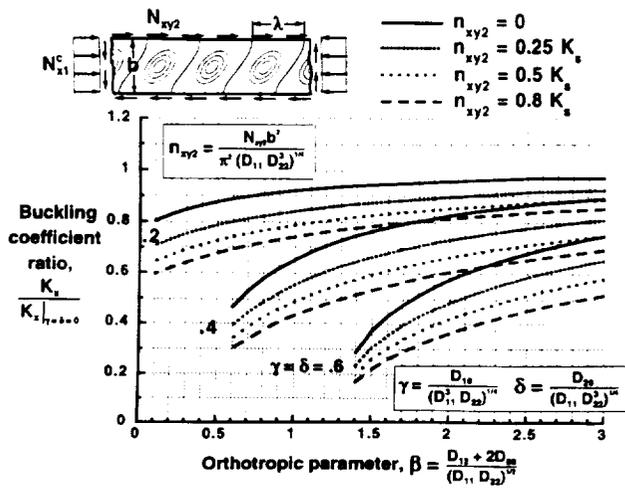
Fig. 15 Effects of orthotropic parameter β and anisotropic parameters γ and δ on buckling coefficients for simply supported plates subjected to axial compression and positive subcritical shear (n_{xy2}) loads.
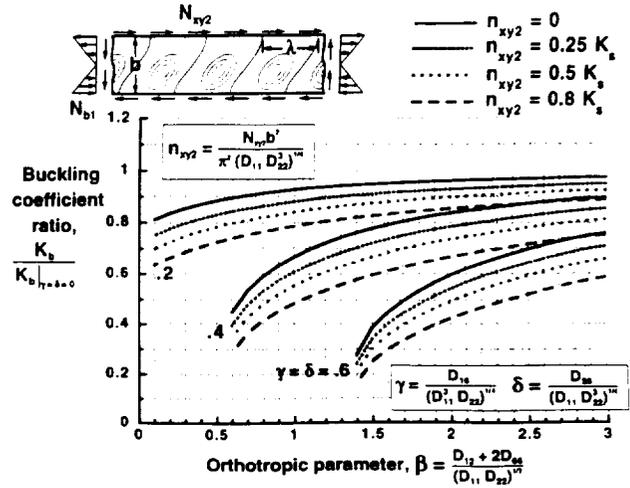

Fig. 17 Effects of orthotropic parameter β and anisotropic parameters γ and δ on buckling coefficients for simply supported plates subjected to pure inplane bending and positive subcritical shear (n_{xy2}) loads.
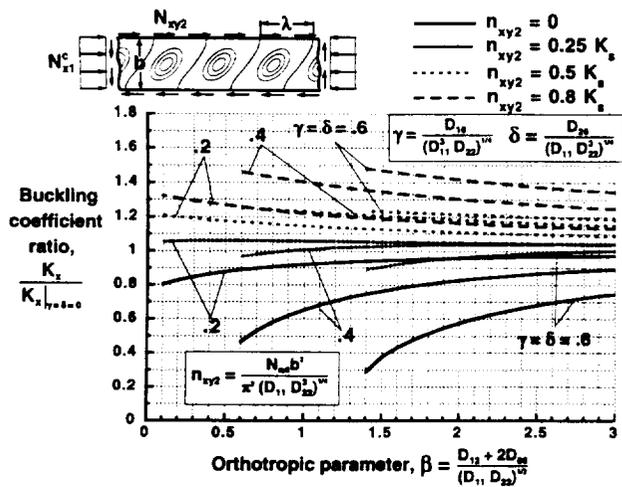
Fig. 16 Effects of orthotropic parameter β and anisotropic parameters γ and δ on buckling coefficients for simply supported plates subjected to axial compression and negative subcritical shear (n_{xy2}) loads.
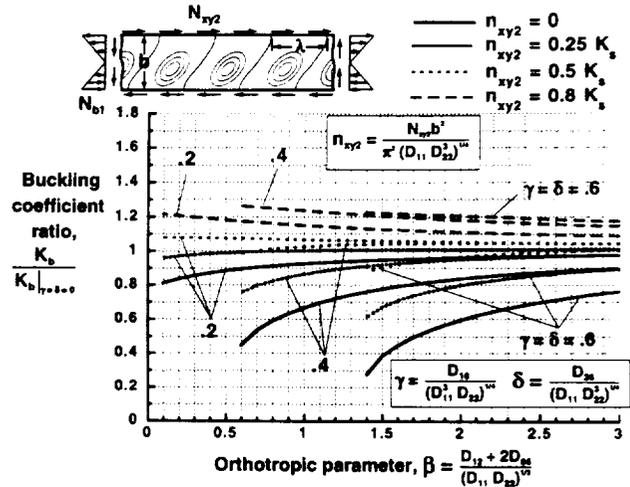

Fig. 18 Effects of orthotropic parameter β and anisotropic parameters γ and δ on buckling coefficients for simply supported plates subjected to pure inplane bending and negative subcritical shear (n_{xy2}) loads.

12